arXiv:0711.4811v1 [astro-ph] 29 Nov 2007

Gravitational Lensing Characteristics of the Transparent Sun

Bijunath Patla and Robert J. Nemiroff
Michigan Technological University, Department of Physics,
1400 Townsend Drive, Houghton, MI 49931

Received ______________________; accepted ______________________

Submitted to: The Astrophysical Journal

ABSTRACT

The transparent Sun is modeled as a spherically symmetric and centrally condensed gravitational lens using recent Standard Solar Model (SSM) data. The Sun's minimum focal length is computed to a refined accuracy of 23.5 ±0.1 AU, just beyond the orbit of Uranus. The Sun creates a single image of a distant point source visible to observers inside this minimum focal length and to observers sufficiently removed from the line connecting the source through the Sun's center. Regions of space are mapped where three images of a distant point source are created, along with their associated magnifications. Solar caustics, critical curves, and Einstein rings are computed and discussed. Extremely high gravitational lens magnifications exist for observers situated so that an angularly small, unlensed source appears near a three-image caustic. Types of radiations that might undergo significant solar lens magnifications as they can traverse the core of the Sun, including neutrinos and gravitational radiation, are discussed.

Subject headings: gravitation – gravitational lensing – solar system: general – Sun: general

1. Introduction

Our Sun is known to act as a gravitational lens. The angular shift of the apparent position of a star located behind the Sun was first observed during the Solar eclipse of 1919 (Dyson, F. W., Eddington, A. S. & Davidson C. 1920), in conformity with the predictions of general relativity (Einstein 1916). Many years later, Einstein (1936) discussed the lens like action of the Sun's gravitational field more generally. The influence of that discussion has caused the ring seen by the observer during perfect alignment of the source, lens and the observer to be called the Einstein ring around a point lens.

For an opaque lens, the result of exterior focusing of the parallel light rays incident with an impact parameter b on the lens plane is a deflection α. The deflection α is inversely proportional to the impact parameter b according to the formula first derived by Einstein (1911)

$$\alpha = \frac{4GM_b}{bc^2}, \tag{1}$$

where b is the impact parameter of the passing light ray, M_b is the deflecting mass, G is the gravitational constant and c is the speed of light in vacuum. Assuming the deflection angle is small, the minimum focal length for the opaque sun is approximated by

$$F_{min} = \frac{R_\odot^2 c^2}{4GM_\odot} = 548.30(\pm.01)\ \mathrm{AU}, \tag{2}$$

where $M_\odot$ and $R_\odot$ are the total mass and radius of the Sun, respectively. The uncertainty in F_{min} is based on statistical errors on $R_\odot$ and $GM_\odot$ (Cox 1999). Slight offsets of the lens or source from the optic axis will break the Einstein ring into two bright images as seen by the observer. Therefore the opaque Sun produces multiple images only beyond F_{min}.

The possibility of using the *transparent* Sun as a gravitational lens was first discussed by Cyranski and Lubkin (1974) and more recently by Nemiroff and Ftaclas (1997). Demkov and Puchkov (2000) computed a minimum focal length of the transparent Sun to be about

24 AU. Starting with the Standard Solar Model as it was known in 1989 (Bahcall 1989), they computed the gravitational lens deflection angle as a function of impact parameter and then approximated this with a Taylor's series near the Sun's center.

Throughout the present analysis, the more recent 2005 Standard Solar Model (SSM) data is used (Bahcall et al. 2005). A more complete model of the gravitational lens characteristics of the transparent Sun is computed, including a more accurate minimum focal length (23.5 ± 0.1 AU), regions of multiple images, and the locations of caustics and critical curves.

The plan of the paper is as follows: § 2 outlines two alternative approaches to obtain the minimal focal length of the transparent Sun. The strength of a composite lens capable of producing multiple images is given a through treatment in § 3. The critical curves, caustics, magnification and multiple image zones are computed in § 4, and conclusions summarized in § 5.

2. Solutions of the Lens equation

It is well known that only a point lens can generate two images in the weak deflection limit (Schneider, Ehlers & Falco 1992). However, a composite lens can produce multiple images. The location of images in the lens plane depends on the enclosed projected mass within the impact radius. Burke's odd number theorem (Burke 1981) states that a composite lens can produce only odd number of images of the source, and the images always appear (disappear) in pairs as the source moves inside (outside) of a caustic.

In the standard geometrical optics approximation, light rays start out straight from a source and then change directions discretely at the deflector plane, subsequently reaching the observer. To utilize geometric optics for a composite lens, one must project the three-dimensional mass of the deflector onto a plane perpendicular to the optical axis connecting the source to the observer. A plane wave approximation is assumed by considering source radiation that has a wavelength $\lambda \ll R_S$, where $R_S = 2GM_\odot/c^2$, is the Schwarzschild radius of the deflecting lens mass.

It is also assumed that the sources are point like and there is no contribution due to internally converging Ricci focusing by the mass within a pencil of rays. In other words the light bundle is assumed to be infinitesimally thin and the deflection is purely due to Weyl focusing by the projected mass lying within the impact radius (Dyer 1977). The mass outside of the impact radius does not contribute to the deflection, following Newton's and Birkhoff's theorem.

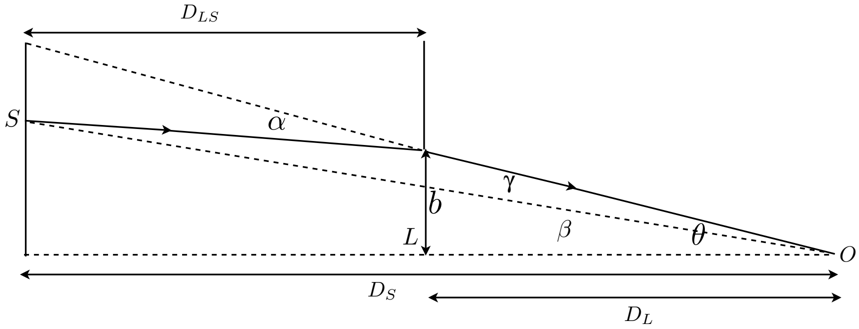

Fig. 1.— The center of the lens L is at a distance D_L from the observer O and a distance D_{LS} from the source S. β and θ are the angles subtended by the unlensed source and its image visible to the observer.

The geometry of Fig. 1 satisfies the equation

$$\vec{\beta} = \vec{\theta} - \vec{\alpha}\frac{D_{LS}}{D_S}. \tag{3}$$

If one considers sources that are very far away, then $D_{LS} \approx D_S$. Hence the lens equation takes a simplified form

$$\vec{\beta} = \vec{\theta} - \vec{\alpha}. \tag{4}$$

In terms on the two dimensional projected density $\Sigma(r)$ of the lens equation (1) can be recast in the form

$$\vec{\alpha} = \frac{4G}{c^2} \int_S r' d\phi dr' \Sigma(r') \frac{\vec{r'}}{|r'|^2}, \tag{5}$$

where $\Sigma(r')$is the value of the projected mass density at the point r' from the center of the lens, r' is the impact parameter, and S the surface area in a polar (r, ϕ) coordinate system . The center of the lens is made to coincide with the center of the preferred coordinate system for simplicity and owing to the cylindrical symmetry. Defining a dimensionless parameter

$$\kappa(r) = \frac{\Sigma(r)}{\Sigma_{cr}}, \tag{6}$$

where Σ_{cr} is the critical density, a reference measure to determine the strength of the lens from an observer's stand point, see for example (Subramanian & Cowling 1986 ; Schneider et al. 1992):

$$\Sigma_{cr} = \frac{c^2}{4\pi G D_L}, \tag{7}$$

where D_L is the distance between the lens and the observer. Using equation (6) and equation (4) in equation (5) and scaling the radial coordinate using the relation, $\theta = r/D_L$, yields

$$\vec{\alpha} = \frac{1}{\pi} \int_S \theta' d\phi d\theta' \kappa(\theta') \frac{\vec{\theta'}}{|\theta'|^2}, \tag{8}$$

where θ' is the angular position of the image, as seen by the observer located at a distance D_L, corresponding to an impact radius r'. A scalar potential $\psi(\vec{\theta})$ can be defined such that,

$$\psi(\vec{\theta}) = \frac{1}{\pi} \int_S \theta' d\phi d\theta' \kappa(\theta') \log |\vec{\theta'}|, \tag{9}$$

where ϕ is the polar angular coordinate. Comparing equation (9) with equation (8) and noting that $\nabla \log |\vec{\theta'}| = \vec{\theta'}/|\vec{\theta'}|^2$,

$$\vec{\alpha} = \nabla_\theta \psi(\vec{\theta}). \tag{10}$$

A generalized lens equation can be obtained by using equation (10) in equation (4):

$$\vec{\beta} = \nabla_\theta \left(\frac{\vec{\theta}^2}{2} - \psi(\vec{\theta}) \right). \tag{11}$$

Essentially equation (11) is a mapping from $\vec{\theta} \rightarrow \vec{\beta}$, as the observer traces the ray back to the source. The numerical solution of equation (11) yields the image locations. The $2D$ potential of the lens plane, then appears in the lens equation as elements of the inverse metric $g^{\alpha\beta}$ (Schneider, et al. 1992). $\psi(\vec{\theta})$ is a function of $\vec{r}$ (radius) only, owing to the circular symmetry. In general it is a function of two parameters of a polar coordinate system. In other words, the source and the image locations do not align on a straight line.

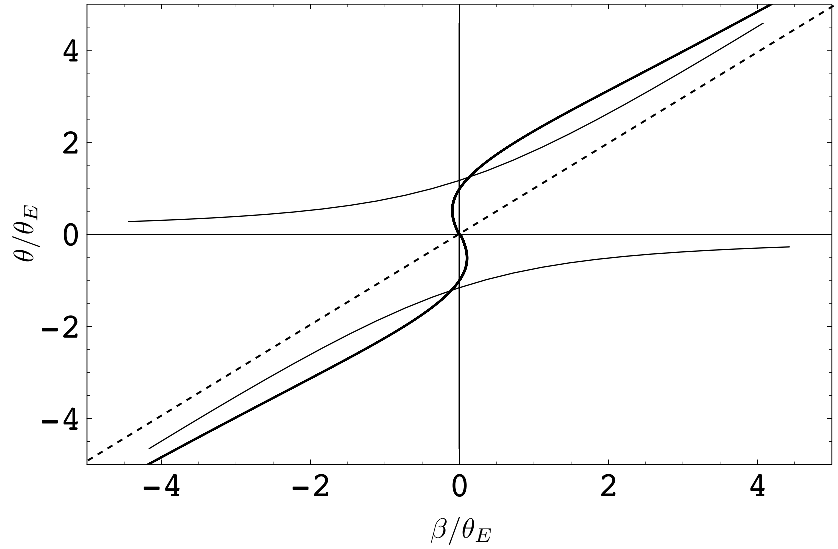

Fig. 2.— The curves relate unlensed source positions β and the image locations θ for three different scenarios. The continuous curve represents the solutions of the lens equation for a centrally condensed lens. The disjoint set of curves delineates a point lens of the same mass and the straight line corresponds to the absence of a lens, where unlensed source positions and image positions coincide at all times.

The solutions to the lens equation have a maximum of three roots. Any vertical line in the $\beta - \theta$ plane corresponds to a fixed source location, the points of intersection of which are the corresponding image locations. Inspection of Fig. 2 shows that sources far from the optic axis are seen as a single image. The $\beta - \theta$ curves are conformal transformations for the mapping $\vec{\theta} \rightarrow \vec{\beta}$ for every observer location D_L. Note that the Fig. 2 is based on an inverted map that is used to calculate the magnification.

At $\beta = 0$ the two images are equally separated from the optic axis. The assumed spherical symmetry of the lens will generate a circular Einstein ring on the lens plane. The formation of a real Einstein ring requires that a source be placed exactly along the line joining the observer through the center of the lens, which, for realistic cases, only occurs for sources of finite size. Nevertheless, an Einstein ring still has theoretical significance since it separates sets of images (Nemiroff 1993). For example, as the source moves behind the lens, no source image will ever be seen to cross an Einstein ring.

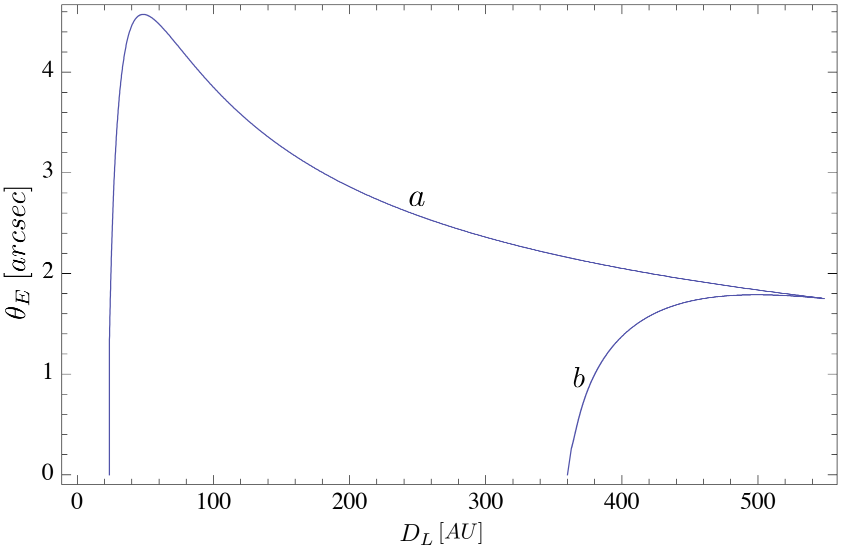

Fig. 3.— The radius of Einstein rings as function of observer–lens distance D_L along the optic axis. The curve (a) corresponds to the Sun and curve (b) corresponds to a homogenous lens with a radius and mean density equal to the Sun. The angle subtended at the limb of the Sun in both cases converge to ≈ 1.75”

It is important to make a distinction between what is meant by focal length for an optical lens as apposed to a gravitational lens. The focal length of an optical lens is the distance between the center of the lens and the point where paraxial light rays converge or appear to diverge. The definition of deflection angle is

$$b = F \tan \alpha, \tag{12}$$

where b, F and α are the impact parameter, focal length and deflection angle respectively.

The gravitational lens has a focal length for each impact parameter bounded by a minimum focal length. This is because the deflection angle is not a linear function of impact parameter. Paraxial light rays converge at different points along the optic axis.

The existence of multiple images is a necessary condition for a consistent definition of focal length. Past the minimum focal length, the observed merger of two source images results in the formation of an Einstein ring. Numerical simulations (discussed more in the Appendix) involving different values of D_L and Burke's odd number theorem will impose the following mathematical condition, for the existence of multiple images (Schneider, et al. 1992):

$$\frac{d\theta}{d\beta} < 0. \tag{13}$$

The least value of D_L that conforms to the above condition, the minimum focal length, is found numerically to be 23.5 AU. This implies that, for values of D_L less than 23.5 AU there are no multiple images and hence no focal point. The perfect alignment of the source, lens and the observer at a distance less than 23.5 AU will not result in the formation of Einstein ring.

3. Strength of a centrally peaked lens

Not only does the Sun's mass density decrease monotonically with radius, but its mass density projected onto a lens plane also decreases monotonically with radius. Surface density normalized to the critical surface density needed to generate multiple images is referred to as a dimensionless surface density κ and is a measure of the strength of the lens (Schneider, et al. 1992). If $\kappa(\vec{r}) \geq 1$ for *some* regions on the lens then the lens is termed "strong." For instructive comparisons to our Sun, a "constant density" sphere of radius $R_\odot$ with a volume density equal to the average density of the Sun is used.

A "weak" lens is characterized by $\kappa(\vec{r}) \ll 1$ and cannot produce multiple images (Subramanian & Cowling 1986). The constant density sphere does not produce multiple images at $D_L = 23.5$ AU. This is illustrated in Fig. 4, where curve (b) has a value of $\kappa(\vec{r}) \ll 1$ throughout the entire the lens at 23.5 AU. Weak lenses are only weak for observers sufficiently close – observers further than some minimal focal length will see the same object as a strong lens that creates multiple images. In case of the constant density sphere of Solar mass, this value for D_L is ~ 360 AU.

The validity of equation (13) implies that, the transition of the lens from being weak to strong should have at least so many points, such that the $\beta - \theta$ curve is continuous at the minimum focal length. Therefore, more than a single method is required to establish and verify the existence of a minimum focal length more precisely, accounting for the less than one percent combined error of the data (Bahcall et al. 2005) and simulations.

Alternatively, the minimum focal length of the Sun can be obtained by using the values of the mass enclosed and the impact parameter corresponding to the value of $\kappa(\vec{r}) = 1$. Using equation (2) and the substituting the value $0.0137 M_\odot$ and the radius of the enclosed mass $.024 R_\odot$ one obtains a focal length of ≈ 23.5 AU, which lies between the orbits of Uranus and Neptune.

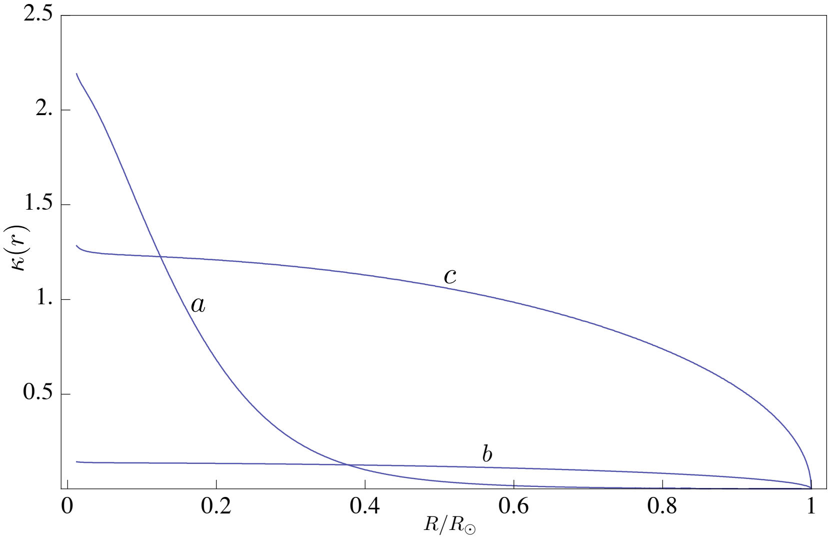

Fig. 4.— The surface density κ plotted on the vertical axis is a monotonically decreasing function of radius. The curves (a) corresponds to the Sun for observer–lens distance $D_L = 50$ AU, whereas curves (b) and (c) represents the homogeneous density sphere at D_L of 50 and 450 AU. The dimensionless surface density parameter suggests that the transparent Sun is a strong lens just above 23.5 AU and a homogeneous model lens is a weak lens $\kappa \ll 1$ at the same D_L. The very same model lens is capable of producing multiple images at observer–lens distance (D_L) greater than 360 AU.

4. Critical curves, caustics and magnification

The lens plane is defined as the plane perpendicular to the line joining a point source and a fixed observer. According to the odd number theorem for transparent gravitational lenses (Burke 1981), the observer will see an odd number of images of the point source no matter what position the center of the lens occupies in the lens plane. Areas might exist in the lens plane where the lens center can be placed to create a specific odd number of images visible to the observer. The boundaries between these areas are called critical curves. For a spherically symmetric lens, a critical curve is a circle. Were a lens center to lie on a critical curve, a formally infinite magnification of a point source would be seen by the observer.

The source plane is defined as a plane perpendicular to the line extending from a fixed observer through the lens center. In analogy with the lens plane, areas might exist in the source plane where a point source can be placed so the (fixed) lens creates a specific odd number of images visible to the (fixed) observer. The boundaries between these areas of the source plane are called caustics. For spherical lenses, the caustics are also circles. Were a point source to lie on a caustic, a formally infinite magnification would be seen by the observer. For a given lens, the θ versus β curve may show points of diverging slope. These points correspond to infinite magnification, and hence yield the angular radii of the corresponding caustic (β) and critical (θ) circles.

Let's now consider specifically our Sun. The θ versus β curve is shown in Fig. 2. At 30 AU, just outside the minimum focal length of 23.5 AU, the radius of the caustic is found to be 10 $\%\theta_E$ where $\theta_E = 3.65$", the angular Einstein ring radius. In terms of the dimensions of the Sun, the radius of the Einstein ring is .1 $R_\odot$ and the caustic is .01 $R_\odot$. Similarly the radius of the critical curve is found to be 50 $\%\theta_E$ or $\approx$ .06 $R_\odot$. Table 1 summarizes the relative radii of Einstein ring, caustic and critical curve for different observer locations. $\theta_\odot$ is the angular measure of the Sun's radius for the corresponding D_L.

The apparent relative motion of an angularly small source behind the Solar lens will

Table 1. Radii of critical curves and caustics

D_L(AU)	$\theta_E/\theta_\odot$	θ_{caus}/θ_E	θ_{crit}/θ_E	$\theta_{caus}/\theta_\odot$	$\theta_{crit}/\theta_\odot$
23.0	0	0	0	0	0
25.0	$5.62\ 10^{-2}$	$3.68\ 10^{-2}$	0.481	$2.07\ 10^{-3}$	$2.70\ 10^{-2}$
27.0	$8.24\ 10^{-2}$	$6.14\ 10^{-2}$	0.518	$5.06\ 10^{-3}$	$4.28\ 10^{-2}$
30.0	0.113	0.100	0.519	$1.13\ 10^{-2}$	$5.87\ 10^{-2}$

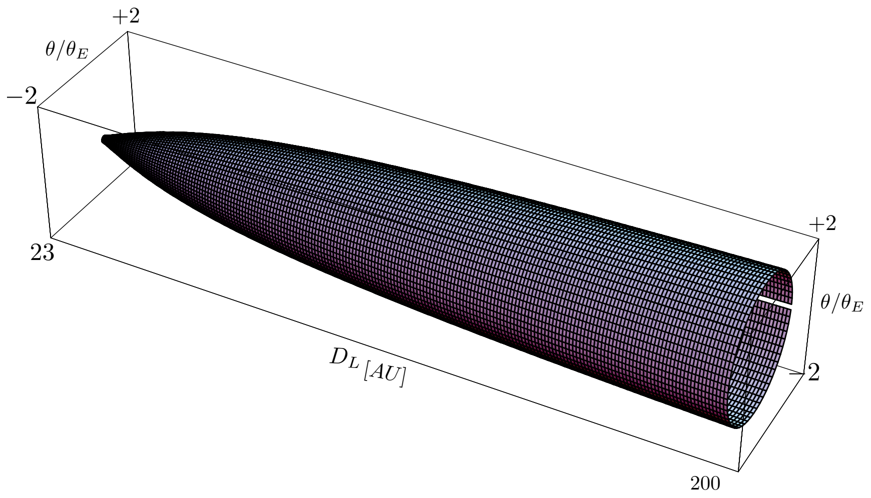

Fig. 5.— The points inside the above surface of revolution represent the volume where an observer sees multiple images. The angular distances are normalized to the units of Einstein ring radii corresponding to a given D_L along the horizontal axis.

result in a light curve with sharp spikes when the source crosses a caustic. The magnification at a given location can be obtained from the $\beta - \theta$ curve corresponding to that location

$$\mu = \frac{\theta}{\beta}\frac{d\theta}{d\beta}. \tag{14}$$

The straight line motion of the source behind a weakly acting lens will result in a light curve which peaks at the minimum distance the source appears from the lens. This minimum angular distance is called the impact parameter, n for the source. The distance separating the projected source on the lens plane and the center of the lens scales as β and the corresponding distance for the single image scales as θ for small β and θ. For large distances of the source from the center of the lens, the image nearly coincides with the source. But, as this distance decreases, the image and the source locations on the lens plane diverge as seen by the observer. For a strong lens, unlensed source positions inside a circular caustic create three images of the source visible to the observer. Regardless of the number

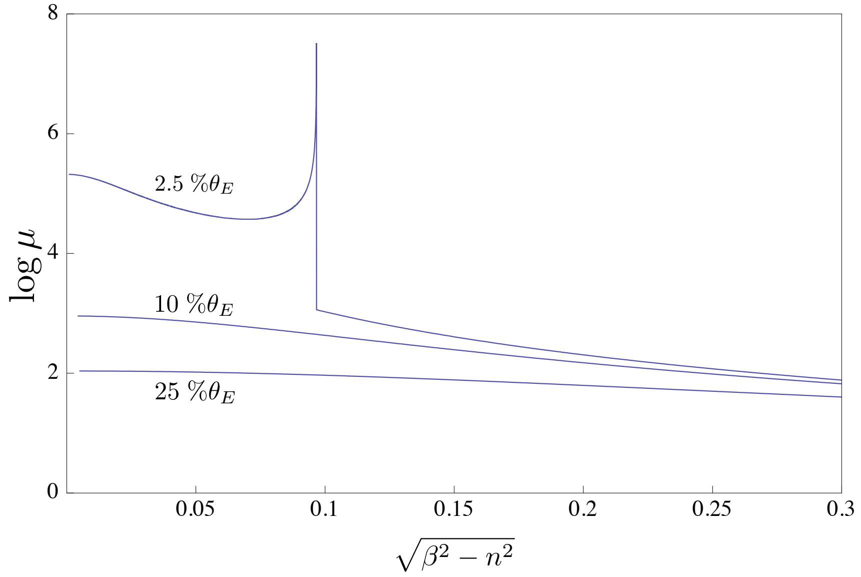

Fig. 6.— The light curve on the top is that of a point source, moving behind the lens with an impact parameter, n, expressed as an angular measure of $2.5\%\theta_E$. As the distance separating the source and the lens increases, a pair of images disappears. The vertical axis is the magnification in logarithmic scale and the horizontal axis represents the distance scale normalized to angular size of the Einstein ring θ_E.

of observed source images, a finite size source will undergo a finite total magnification.

Large magnifications allows us a more sensitive look for neutrino flux from nearby stars, as well as high energy gravitational radiation. The gravitational radiation with the wavelength of $\approx km$ will be lensed by the sun (Isaacson 1968; Thorne 1989). In order to satisfy plane wave approximation and to account for diffraction effects, the characteristic length scale, $\approx$ Schwarzschild radius of the Sun puts an upper limit on the wavelengths of detectable gravitational wave spectrum.

High energy neutrinos, by definition, have energies greater than 100 GeV(Gaisser, Halzen & Stanev 1995). The Sun admits neutrinos, unimpeded by electron scattering, only for energies up to 300 GeV(Escribano et al. 2001). So, unlike gravitational waves, the neutrino spectrum is primarily low energy. The mass distribution of the Sun within the impact radius that allows for a minimum focal length, puts an upper limit on the neutrino energy spectrum.

5. Discussion

The effects of plasma and core rotation in the interior of the Sun, thought to be small, were ignored during this analysis. The minimum focal length, the critical curve and caustics were computed numerically. The magnification of point sources for typical source separations was analyzed. The code can be modified to simulate galaxies and dark matter halos with an assumed density profile as input parameters.

To date, four spacecraft have traveled past the minimum transparent focal length of our Sun, just beyond the orbit of Uranus. Launching a spacecraft to this distance with sufficiently sensitive gravitational wave or neutrino detectors remains a dream, however. In a different paper, the possibility of detecting strong gravitational radiation and a wide range of neutrino energy spectrum will be examined in some detail. With the advancement of modern technology and the improvement in the resolution power of detectors, such an endeavor could shed new light on sources emitting neutrinos, high energy gravitational waves or hitherto hypothetical particles that are predictions of at least some theories.

A. Appendix

The image locations for a given impact parameter are found by solving equation (4. By allowing for a range of both positive and negative values for the deflection angle α for all positive values of source position β, and interpolating within bounds, one obtains the image locations θ. Therefore, this can be termed as a controlled ray tracing algorithm

$$\beta = \frac{b}{D_L}, \tag{A1}$$

where b, and D_L are the impact parameter and fixed observer distance from the lens' center. The resulting curve is shown in Fig. 2. For point sources the magnification can be computed directly from the curves using equation (14). Magnifications for extended sources can be computed by taking the average magnifications of individual randomly generated points, lying within a circle or by choosing neighboring points and taking the ratio of their areas in the lens plane and source planes.

For a circularly symmetric lens, the deflection depends only on the impact parameter. In that case, a new angular measure n can be defined as in Fig. 7, the perpendicular distance from the source on the lens plane. The observer can choose a coordinate system with her y coordinate and origin made to coincide with $\vec{n}$ through the center of the lens. Now at different source positions, as seen by the observer, the source will subtend an angular measure

$$x = \sqrt{\beta^2 - n^2}, \tag{A2}$$

from the x axis, where $\beta \geq n$.

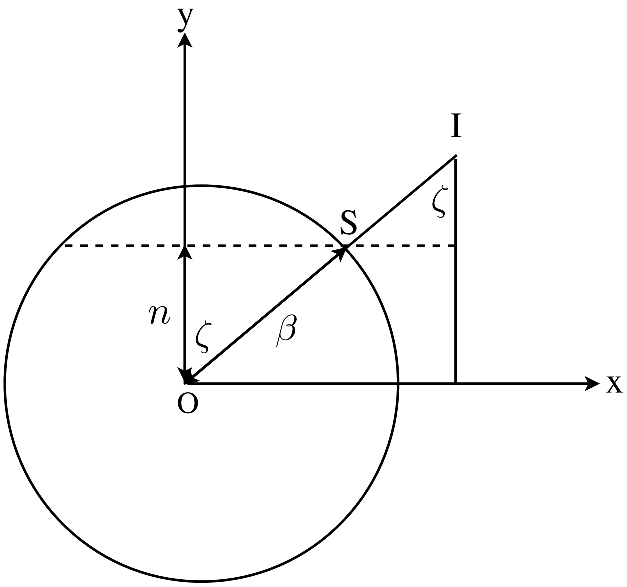

Fig. 7.— The dashed line is the trajectory of the source (S) behind the lens, making an impact parameter n. The image (I) and the source always lies along a straight line for a spherical symmetric lens. Therefore, the angular distance of the source from the center of the lens along the source trajectory, as seen by the observer at any given time is $\sqrt{\beta^2 - n^2}$

REFERENCES

Bahcall, J. N. 1989, Neutrino Astrophysics, (Cambridge: Cambridge University Press)

Bachall, J. N. et al. 2005 , ApJ, 621, L85

Burke, W. L. 1981, ApJ, 244, L1

Cox, A. 1999, Astrophysical Quantities (4th ed.; New York: Springer)

Cyranski, J. F. & Lubkin, E. 1974, Annals of Physics, 87, 205

Demkov, Yu. N. & Puchkov, A. M. 2000, Phys. Rev. D, 61, 083001-1

Dyer, C. C. 1977, MNRAS, 180, 231

Dyson, F. W., Eddington, A. S. & Davidson C. 1920, Philos. Trans. Royal Soc. London, 220A, 291

Einstein, A. (1911)1994, in The Collected Papers of Albert Einstein, Vol. 3 (Princeton: Princeton University Press), 379

Einstein, A. (1916)1997, in The Collected Papers of Albert Einstein, Vol. 6 (Princeton: Princeton University Press), 147

Einstein, A. 1936, Science, 84, 506

Escribano, R., Frere, J. M., Monderen, D. & Van Elewyck, V. 2001, Phys. Lett., B512, 8

Gaisser, T.K., Halzen, F. & Stanev, T. 1995, Phys. Rept., 258, 173; Erratum: 1996, 271, 355

Isaacson, R. A. 1968, Phys. Rev., Vol. 166, No. 5, 1263

Narayan, R. & Bartelmann, M. 1996, preprint (astro-ph/9606001)

Nemiroff, R. J. 1993, American Journal of Physics, 61, Issue 7, 619

Nemiroff, R. J. & Ftaclas, C. 1997, BAAS, 190, 38.01

Schneider, P., Ehlers, J., & Falco, E. E. 1992, Gravitational Lenses (Berlin: Springer-Verlag)

Subramanian, K. & Cowling, S. A. 1986, MNRAS, 219, 333

Thorne, K. S. 1989, in 300 years of Gravitation, ed. Hawking, S. & Israel,W. (Cambridge: Cambridge University Press), 330

This manuscript was prepared with the AAS LaTeX macros v5.2.